

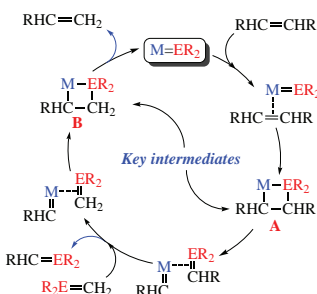
# Group 4 metal silylenes and germylenes: towards the silicon and germanium variations of olefin metathesis

Vladimir Ya. Lee

Department of Chemistry, Faculty of Pure and Applied Sciences, University of Tsukuba, Tsukuba 305-8571, Ibaraki, Japan. E-mail: [leevya@chem.tsukuba.ac.jp](mailto:leevya@chem.tsukuba.ac.jp)

DOI: 10.1016/j.mencom.2023.02.001

The current progress in the field of the stable Schrock-type silylenes and germylenes of the group 4 metals, along with their prospective use in the development of the silicon or germanium variations of olefin metathesis, is briefly overviewed in this focus article.



**Keywords:** germanium, germylenes, metathesis, Schrock complex, silicon, silylenes.

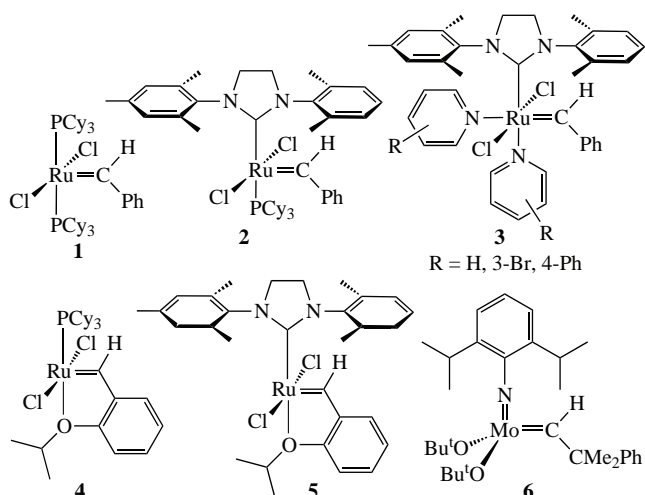
*This paper is dedicated to the anniversary of Professor Irina Beletskaya, academician of the Russian Academy of Sciences, outstanding organic and organometallic chemist.*

## 1. Introduction

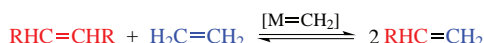
The formation of carbon–carbon bonds is one of the ultimate goals of organic chemistry critically important in many applied fields, for example, in the synthesis of biologically active compounds including pharmaceuticals and natural products. Olefin metathesis, involving redistribution of fragments of two olefins by the cleavage and reformation of the C=C double bonds and catalyzed by the transition metal carbene complexes (Scheme 1),<sup>1–6</sup> is among the most powerful methods for the catalytic carbon–carbon bond formation with many critically important industrial applications, such as Shell Higher Olefins Process (SHOP),<sup>7</sup> Olefins Conversion Technology (OCT),<sup>7</sup> and natural product synthesis.<sup>8</sup>

There are two distinct classes of well-defined homogeneous catalysts for olefin metathesis of the type [M=CH<sub>2</sub>], Grubbs carbene complexes and Schrock alkylidenes, both of which being commercialized in 1990s and successfully applied for industrial fine chemical synthesis. A family of the ruthenium-

based Grubbs catalysts includes [Cl<sub>2</sub>(Cy<sub>3</sub>P)<sub>2</sub>Ru=CHPh] **1** (1<sup>st</sup> generation),<sup>9,10</sup> [Cl<sub>2</sub>(Cy<sub>3</sub>P)(NHC)Ru=CHPh] **2** [NHC = 1,3-bis-



**Scheme 2** Olefin metathesis catalysts: Grubbs catalysts **1–5** and Schrock catalyst **6**.



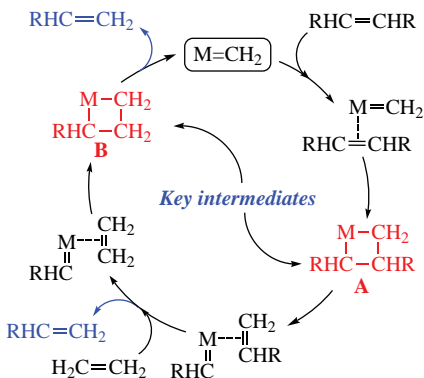
**Scheme 1** Olefin metathesis process: a general scheme.



**Vladimir Ya. Lee** has earned his PhD degree from the N. D. Zelinsky Institute of Organic Chemistry, Academy of Sciences of the USSR. Following two postdoctoral stints, he currently holds a permanent post at the University of Tsukuba (Tsukuba, Japan). His career in the field of Main Group chemistry has spanned a period of over 30 years, with a predominant focus on the study (both experimental and computational) of the low-coordinate derivatives of the Main Group elements: cations, radicals, anions, carbenes, multiply bonded species, aromatic compounds, clusters, and their transition metal complexes (as potential catalysts in the metathesis and cross-coupling reactions).

(2,4,6-trimethylphenyl)dihydroimidazole **2** (2<sup>nd</sup> generation),<sup>11</sup> [Cl<sub>2</sub>(RH<sub>4</sub>C<sub>5</sub>N)<sub>2</sub>(NHC)Ru=CHPh] [R = H, 3-Br, 4-Ph; NHC = 1,3-bis(2,4,6-trimethylphenyl)dihydroimidazole] **3** (3<sup>rd</sup> generation),<sup>12</sup> and Hoveyda–Grubbs catalysts **4** (1<sup>st</sup> generation)<sup>13</sup> and **5** (2<sup>nd</sup> generation) featuring a chelating *ortho*-isopropoxy group attached to the benzene ring (Scheme 2).<sup>14,15</sup> The Schrock catalysts of the type {(Bu<sup>1</sup>O)<sub>2</sub>[(2,6-Pr<sup>1</sup>C<sub>6</sub>H<sub>3</sub>)N=]Mo=CHCMe<sub>2</sub>Ph} **6** are generally based on molybdenum (Scheme 2).<sup>16</sup> Although Schrock complexes are typically more reactive than their Grubbs congeners, the latter are more air-stable and advantageously tolerate many functional groups in the alkene substrates.

The commonly accepted mechanism of olefin metathesis was proposed for the first time by Chauvin *et al.* (Scheme 3).<sup>17</sup>

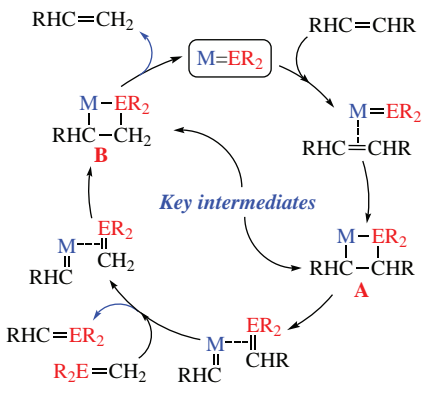


**Scheme 3** Chauvin's catalytic cycle for the olefin metathesis (M = transition metal).

The catalytic cycle involves initial [2+2] cycloaddition of a starting alkene RHC=CHR and a transition metal alkylidene [M=CH<sub>2</sub>] as a catalyst to form metallacyclobutane **A** as a key reaction intermediate. Cycloelimination of **A** generates a new alkene RHC=CH<sub>2</sub> and a new alkylidene [M=CHR], with the latter undergoing [2+2] cycloaddition of a second starting alkene H<sub>2</sub>C=CH<sub>2</sub> forming new metallacyclobutane **B**. Subsequent cycloelimination of **B** forms another equivalent of a new alkene RHC=CH<sub>2</sub> and regenerates catalyst [M=CH<sub>2</sub>].

The yet unknown silicon or germanium versions of metathesis are highly desirable providing unprecedented general access to metallaalkenes of the type RHC=ER<sub>2</sub> (Scheme 4) that can serve as indispensable source for advanced materials of the new generation (Si/Ge polymers, ceramics, films, coatings, nanocomposites, *etc.*).

One can propose a catalytic cycle for the hypothetical Si/Ge-versions of metathesis (see Scheme 4) based on the classical olefin metathesis process (see Scheme 3), being catalyzed by the

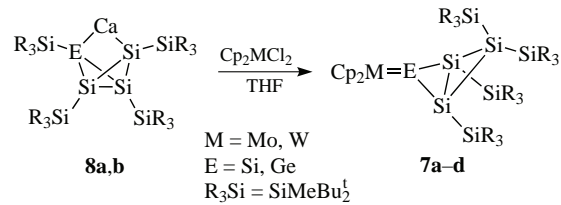


M = transition metal; E = Si, Ge

**Scheme 4** Catalytic cycle for the hypothetical Si/Ge-version of olefin metathesis.

transition metal silylenes or germylenes M=SiR<sub>2</sub> or M=GeR<sub>2</sub>, respectively. However, this highly attractive synthetic approach towards otherwise hardly available metallaalkenes RHC=ER<sub>2</sub> is actually exceptionally challenging. The major hurdle is the structure of the synthetically available 18-electron silylene or germylene complexes M=ER<sub>2</sub> (M = transition metal, E = Si or Ge), which in the overwhelming majority of cases are coordinatively saturated lacking a vacant coordination site and thus being incapable of activation of an unsaturated substrate, as a prerequisite of the first mandatory step of [2+2] cycloaddition to form metallacyclobutane (see Scheme 4).<sup>18–23</sup> As practically all of the above-mentioned silylene and germylene complexes M=ER<sub>2</sub> (E = Si or Ge) of the mid- (groups 5–7) and late (groups 8–11) transition metals M were recently categorized as the Fischer-type complexes,<sup>23</sup> one can conclude that the Fischer silylene and germylene complexes are reluctant towards the [2+2] cycloadditions and accordingly have rather limited prospects as initiators for the Si/Ge-versions of metathesis. As the only exception, there was one recent report of some [2+2] cycloaddition reactions of the Fischer-type (amido)(chloro)silylene–Ni<sup>0</sup> complex {[2,6-Pr<sup>1</sup>C<sub>6</sub>H<sub>4</sub>](Me<sub>3</sub>Si)N](Cl)Si→Ni(NHC)<sub>2</sub>} (NHC = C[(Pr<sup>1</sup>)NC(Me)]<sub>2</sub>) and unsaturated organic substrates.<sup>24</sup>

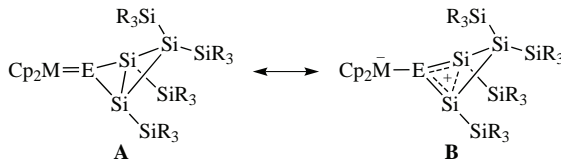
As a representative example, one can mention base-free molybdenum and tungsten silylene and germylene complexes {Cp<sub>2</sub>M=E[Si<sub>3</sub>(SiMeBu<sup>1</sup>)<sub>4</sub>]} **7a–d** (a M = Mo, E = Si; **b** M = Mo, E = Ge; **c** M = W, E = Si; **d** M = W, E = Ge), reported by Lee, Sekiguchi and coworkers.<sup>25,26</sup> These bicyclic silylene and germylene complexes **7a–d** were readily prepared by the reaction of the calcium salt of tetrasila- **8a** (E = Si) and trisilagermabicyclo[1.1.0]butane-2,4-diide **8b** (E = Ge) with molybdenocene and tungstenocene dichlorides (Scheme 5).



**Scheme 5** Synthesis of the base-free molybdenum and tungsten silylene and germylene complexes **7a–d**.

As is diagnostic for the base-free silylene complexes, both **7a** and **7c** revealed an exceptional deshielding of their sp<sup>2</sup>-Si centers with chemical shift observed at 323.6 and 260.9 ppm [<sup>1</sup>J(<sup>29</sup>Si–<sup>183</sup>W) = 278.2 Hz], respectively.<sup>25</sup> This points, along with the peculiar structural features of **7c** (stretching of the W=Si double bond [2.4202(14) Å], shortening of the cyclic Si<sub>W</sub>–Si bonds [2.3290(18) and 2.3231(19) Å], and elongation of the bridging Si–Si bond [2.4170(16) Å]), to an important contribution of the zwitterionic resonance structure **7B**, in which the bond between the transition metal M and heavy tetrel E is polarized as M<sup>–</sup>=E<sup>+</sup> and the positive charge on E is further delocalized over the ESi<sub>2</sub>-ring, thus forming the homoaromatic cyclobutenium-type system (Scheme 6).<sup>24</sup>

Accordingly, **7a–d** should be recognized as 18-electron Fischer-type silylene and germylene complexes that are



**Scheme 6** The two resonance extremes for the molybdenum and tungsten silylene and germylene complexes **7a–d**: neutral **A** and zwitterionic **B** (E = Si, Ge).

coordinatively saturated and accordingly failed to produce the expected [2+2] cycloadducts with terminal alkynes.<sup>25,26</sup>

As the Fischer-type silylene and germylene transition metal complexes were unable to react with unsaturated hydrocarbons forming the desired metallacycles as the first step of metathesis catalytic cycle, for the realization of silicon or germanium versions of olefin metathesis the Schrock-type silylenes and germylenes were targeted.

## 2. Group 4 metal silylenes and germylenes

Unlike Schrock alkylidenes which are commonly found among the carbene complexes of the group 4–7 transition metals, of all silylene and germylene complexes of the early and mid-transition metals only those of group 4 are reliably classified as the Schrock-type silylenes and germylenes.<sup>23</sup> These will be briefly discussed below along with the prospects of their potential use as the initiators in the silicon or germanium variations of metathesis.

### 2.1. Group 4 metal silylenes

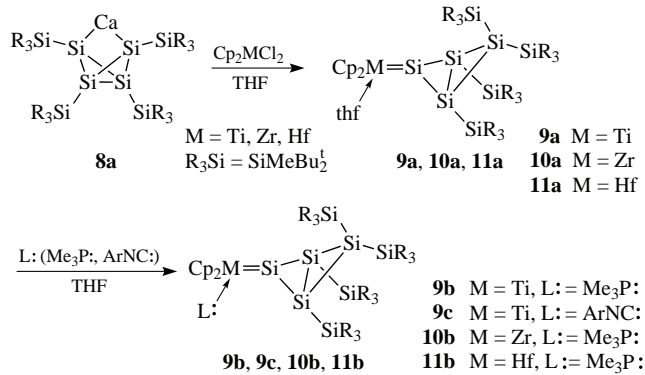
#### 2.1.1. Titanium silylenes Ti=Si

The nature of the multiple bonding and the strength of the Ti=Si double bond was computationally approached a couple of decades ago by Chung and Gordon.<sup>27</sup> At the highest (at that time) level of theory MRMP2/TZVP, the multi-configurational self-consistent field study disclosed the Ti=Si bond dissociation energy of 56.9 kcal mol<sup>-1</sup>.

However, the experimental realization of the titanium silylene complexes lagged behind the theoretical predictions. Accordingly, only in a few publications the synthesis of the titanium silylene complexes was reported. Thus, Driess, Inoue and co-workers reported bis(silylene) titanium(II) complexes  $\text{Cp}_2\text{Ti}(\text{NHSi})_2$  ( $\text{Cp} = \eta^5\text{-C}_5\text{H}_5$ ,  $\text{NHSi} = \text{cyclo-}[\text{Si}(\text{R})(\text{NBu}^t)(\text{CPh})(\text{NBu}^t)]$ ,  $\text{R} = \text{Cl, Me, H}$ ), synthesized by the ligand exchange of  $\text{Cp}_2\text{Ti}(\text{PMe}_3)_2$  and  $\text{NHSi}$  ( $\text{R} = \text{Cl}$ ) and featuring titanium–silicon bond lengths of 2.486(1) and 2.515(1) Å.<sup>28</sup> Based on the peculiar features of the titanium–silicon bond [distorted-tetrahedral geometry at the silicon centers, calculated Wiberg bond index (WBI) values close to unity (0.999–1.0455)], the titanium–silicon interaction in these complexes is best described as a dative single bond, rather than a multiple bond. Moreover, the Ti–Si bond is remarkably polarized towards the transition metal: Natural Population Analysis (NPA) atomic charges for titanium are ranging from -1.279 to -1.328 and those for silicon are ranging from +1.169 to +1.585. This testifies for the predominant contribution of the  $\sigma$ -bonding from the silylene to the titanium center with less important contribution of the  $\pi$ -back-bonding from the metal to the silylene ligand, which in turn allows classification of these coordination compounds as the Fischer-type titanium silylene complexes.

The first (and still the only known) titanium silylene complexes of the Schrock-type, that is titanium silylenes, were reported in 2013 by Lee, Sekiguchi and co-workers.<sup>29</sup> The first in this series, titanium silylene complex  $\{\text{Cp}_2\text{Ti}(\text{thf})=\text{Si}[\text{Si}_3(\text{SiMeBu}^t_2)_4]\}$  **9a**, featuring THF-molecule coordinated to the Ti center, was readily available by the reaction of the above-mentioned calcium salt of tetrasilabicyclo[1.1.0]-butane-2,4-diide **8a** with titanocene dichloride (Scheme 7,  $\text{M} = \text{Ti}$ ).

Being stable in the solid state for a short time, 18-electron THF-complex **9a** unavoidably decomposed in solution *via* the loss of the loosely bound THF-ligand followed by the complete dissociation of the Ti=Si bond in the resulting 16-electron complex  $\{\text{Cp}_2\text{Ti}=\text{Si}[\text{Si}_3(\text{SiMeBu}^t_2)_4]\}$ . Use of trimethylphosphine or xyllyl isocyanide, as the Lewis bases that are remarkably stronger than THF, allowed isolation of the 18-electron titanium



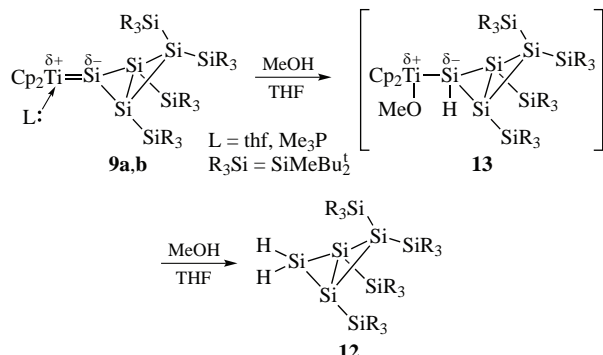
**Scheme 7** Synthesis of the titanium silylene complexes **9a–c**, zirconium silylene complexes **10a,b**, and hafnium silylene complexes **11a,b**.

silylene complexes  $\{\text{Cp}_2\text{Ti}(\text{PMe}_3)=\text{Si}[\text{Si}_3(\text{SiMeBu}^t_2)_4]\}$  **9b** and  $\{\text{Cp}_2\text{Ti}(\text{NCXyl})=\text{Si}[\text{Si}_3(\text{SiMeBu}^t_2)_4]\}$  **9c**, indefinitely stable both in the solid state and in solution [see Scheme 7,  $\text{M} = \text{Ti}$ ,  $\text{L:} = \text{Me}_3\text{P}$ : (for **9b**);  $\text{M} = \text{Ti}$ ,  $\text{L:} = \text{ArNC}$ : (for **9c**)].<sup>29</sup> All complexes **9a–c** revealed extreme deshielding of their doubly-bonded Si centers: 322.4 ppm (for **9a**), 350.6 ppm (for **9b**), and 401.4 ppm (for **9c**). Moreover, there was a remarkable increase in the deshielding (especially on going from **9b** to **9c**), which well agrees with the increase in the same direction of the  $\pi$ -acceptor power of the Lewis base ligand.

In both **9b** and **9c**, the titanium–silicon bonds of 2.5126(6)/2.5099(6) Å (for two crystallographically independent molecules) and 2.5039(6) Å, respectively, are notably shorter than the reported Ti–Si single bonds in silyltitanium complexes (2.59–2.70 Å).<sup>29</sup> In accord with the formulation of these bonds as the double bonds, the Si centers in both **9b** and **9c** are trigonal-planar with the sum of the bond angles around silicon centers ( $\Sigma_{\text{Si}}$ ) of 360.0/359.6° (for two crystallographically independent molecules) and 359.6°, respectively.

The  $d_{\pi}(\text{Ti})-p_{\pi}(\text{Si})$  orbital interaction, as an intrinsic feature of the Ti=Si double bond in **9a–c**, is visualized in their HOMO and LUMO represented by the bonding and antibonding combinations of the 3d(Ti) and 3p(Si) orbitals. NPA charge calculation in **9a–c** showed a strong polarization of the titanium–silicon bond as  $\text{Ti}^{\delta+}=\text{Si}^{\delta-}$ , as is diagnostic for the Schrock alkylidenes, namely: Ti center is positively polarized (+0.78 in **9a**, +0.52 in **9b**, and +0.46 in **9c**), whereas the Si center is polarized negatively (-0.13 in **9a**, -0.08 in **9b**, and +0.01 in **9c**).<sup>29</sup> Thus, based on their spectroscopic, structural, and computational studies, the titanium silylene complexes **9a–c** can be reliably classified as the Schrock-type silylenes, manifesting remarkably nucleophilic Si center and electrophilic  $\text{Ti}^{\text{IV}}$  center in its highest oxidation state  $d^0$ .

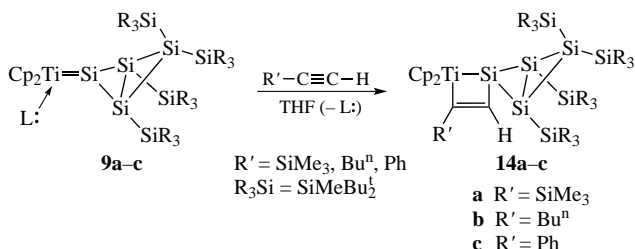
In accord with their  $\text{Ti}^{\delta+}=\text{Si}^{\delta-}$  Schrock-type bond polarization, both **9a** and **9b** selectively reacted with methanol to produce 1,2,2,3-tetrakis(di-*tert*-butylmethylsilyl)tetrasilabicyclo[1.1.0]-



**Scheme 8** Regioselective reaction of the titanium silylenes **9a,b** with MeOH forming tetrasilabicyclo[1.1.0]butane derivative **12**.

butane **12** as a single isolable reaction product (Scheme 8).<sup>23,30</sup> The exclusive formation of **12** is in line with the initial 1,2-addition of MeOH across the  $\text{Ti}^{\delta+}=\text{Si}^{\delta-}$  double bond in accord with its polarization generating intermediate methoxy-derivative **13** with the same  $\text{Ti}^{\delta+}=\text{Si}^{\delta-}$  bond polarization that adds another molecule of methanol, resulting in a complete cleavage of the titanium–silicon  $\sigma$ -bond and formation of the final product **12**.

Titanium silylenes **9a–c** also smoothly reacted with the terminal alkynes  $\text{R}'-\text{C}\equiv\text{C}-\text{H}$ , cleanly and selectively forming the corresponding [2+2] cycloadducts of the  $\text{Ti}=\text{Si}$  and  $\text{C}\equiv\text{C}$  bonds, namely silatitanacyclobutenes **14a–c**, accompanied by elimination of the Lewis base ligand L: (Scheme 9).<sup>29</sup>



**Scheme 9** [2+2] Cycloaddition of the titanium silylenes **9a–c** and terminal alkynes  $\text{R}'-\text{C}\equiv\text{C}-\text{H}$  forming silatitanacyclobutenes **14a–c**.

It should be noted that such [2+2] cycloadditions involving unsaturated hydrocarbons were unprecedented for silylene complexes. There was only one report of the formal [2+2] cycloaddition of the highly polar isocyanate substrate and cationic ruthenium silylene complex, proceeding *via* a different stepwise mechanism initiated by the coordination of the isocyanate nitrogen lone pair to the electrophilic silicon and involving polar intermediates.<sup>31</sup>

Theoretical calculations revealed the exceptional ease of these cycloadditions forming metallacycles **14a–c**, which are highly exergonic ( $\Delta G = -14.6 \text{ kcal mol}^{-1}$  for **14a**) proceeding with practically no activation barrier ( $<1.8 \text{ kcal mol}^{-1}$ ). Computations also showed that on approaching alkyne and 16-electron titanium silylidene  $\{\text{Cp}_2\text{Ti}=\text{Si}[\text{Si}_3(\text{SiMeBu}_2^t)_4]\}$  towards each other,  $d(\text{Ti})$  and  $\pi^*(\text{C}\equiv\text{C})$  orbitals begin to interact at the activation step of the reaction (Figure 1).<sup>29</sup> Such alkyne coordination at Ti is enabled by the preliminary elimination of the Lewis base ligand L: from **9a–c** providing a vacant coordination site at the titanium center, as the prerequisite for the subsequent [2+2] cycloaddition.

The structures of the silatitanacyclobutenes **14a–c** are noteworthy.<sup>29</sup> Thus, in **14a**, the geometry at the spiro-Si atom

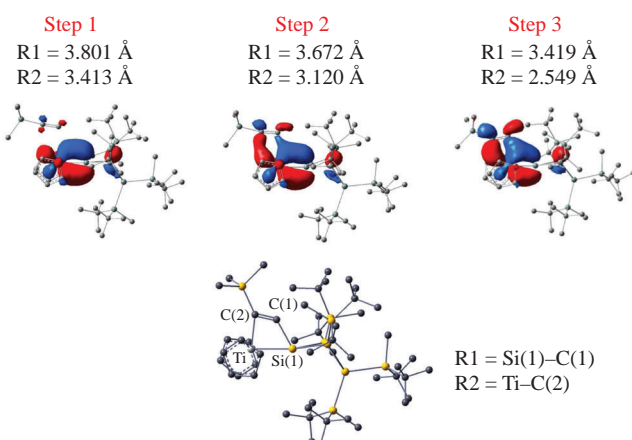


**Figure 1** HOMOs of the reaction system formed upon approaching  $\text{Me}_3\text{Si}-\text{C}\equiv\text{C}-\text{H}$  and titanium silylidene  $\{\text{Cp}_2\text{Ti}=\text{Si}[\text{Si}_3(\text{SiMeBu}_2^t)_4]\}$  towards each other to form metallacycle **14a**.

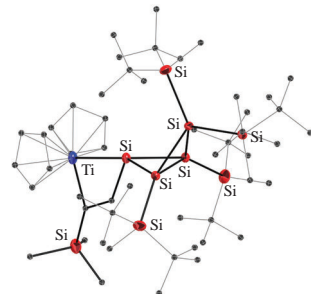
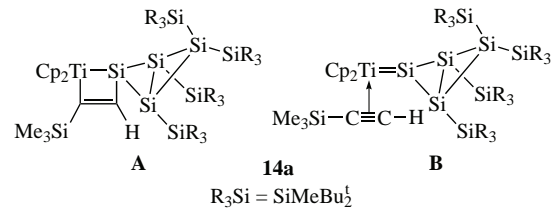


**Figure 2** Crystal structure of the silatitanacyclobutene **14a**.

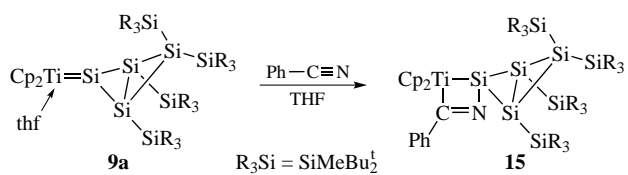
(ignoring olefinic fragment) is essentially planar (Figure 2). The  $\text{Si}-\text{C}$  bond in the  $\text{TiSi}_2$ -ring is notably stretched [2.030(3) Å], whereas the  $\text{Ti}-\text{Si}$  [2.4868(8) Å] and  $\text{C}=\text{C}$  [1.324(4) Å] bonds are shortened, moreover, the diagonal  $\text{Ti}\cdots\text{C}$  interatomic distance [2.319(3) Å] is substantially short indicative of their distant through-space interaction. All these structural features of **14a**, along with its unusually deshielded Ti-bound spiro-Si atom (125.4 ppm), point to the equally important (if not predominant) contribution to the overall composition of the [2+2] cycloadduct **14a** of another resonance extreme **B**, which has the character of a titanium silylidene–alkyne  $\pi$ -complex (Scheme 10).



**Scheme 10** Two major resonance contributors to the overall structure **14a**: metallacycle (**A**) and  $\pi$ -complex (**B**).

Unsubstituted alkyne  $\text{H}-\text{C}\equiv\text{C}-\text{H}$  also readily reacts with the titanium silylidene THF-complex **9a** to form the corresponding silatitanacyclobutene, which is better described as the metallacycle rather than the  $\pi$ -complex, in contrast to the above-discussed case of terminal alkynes  $\text{R}-\text{C}\equiv\text{C}-\text{H}$ .<sup>32</sup>

Likewise, azasilatitanacyclobutene **15**, as a [2+2] cycloadduct of the titanium silylidene **9a** and benzonitrile  $\text{PhC}\equiv\text{N}$ , also revealed properties of a metallacycle rather than a  $\pi$ -complex (Scheme 11).<sup>33</sup> As in the case of the [2+2] cycloadducts with the terminal alkynes **14a–c**, cycloadduct **15** was exclusively formed as a single regiosomer, in which C is bound to Ti and N is bound to Si, which was explained by the steric effects.



**Scheme 11** [2+2] Cycloaddition of the titanium silylidene **9a** and benzonitrile to form azasilatitanacyclobutene **15**.

### 2.1.2. Zirconium silylenes $\text{Zr}=\text{Si}$

Only one compound featuring  $\text{Zr}=\text{Si}$  double bond, zirconium silylene complex  $\{\text{Cp}_2\text{Zr}(\text{thf})=\text{Si}[\text{Si}_3(\text{SiMeBu}_2^t)_4]\}$  **10a** ( $\text{M} = \text{Zr}$ ) was synthesized by the same procedure as used for the preparation of its titanium congener **9a**, namely by the reaction of the calcium salt **8a** with zirconocene dichloride (see Scheme 7).<sup>23,30</sup> Following the general trend of increasing stability of silylene complexes descending group 4, zirconium THF-complex **10a** was stabilized compared to its titanium analogue **9a** to the extent that allowed its isolation and full characterization. As in the

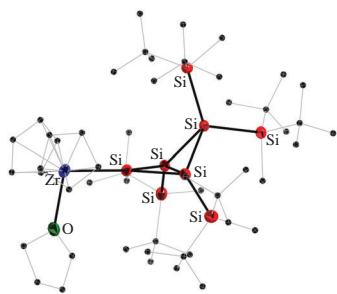


**Figure 3** Crystal structure of the zirconium silylene THF-complex **10a**.

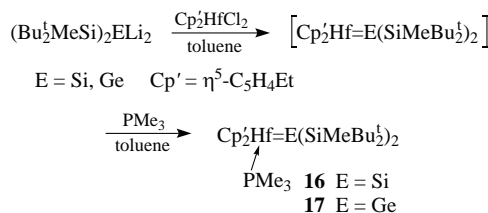
above-described titanium silylidene **9a**, in the zirconium silylene complex **10a**  $sp^2$ -Si center was exceptionally deshielded (248.2 ppm). Preliminary crystallographic data showed that the Zr=Si double bond in **10a** is greatly shorter than the Zr–Si single bonds in zirconocene complexes featuring silyl ligands, and the silylene center is practically planar (Figure 3).

The interaction of the calcium salt **8a** with zirconocene dichloride bearing Et-substituted cyclopentadienyl ligand  $Cp'$  ( $Cp' = \eta^5-C_5H_4Et$ ) also produced the corresponding zirconium silylene complex  $\{Cp'_2Zr(\text{thf})=\text{Si}[Si_3(\text{SiMeBu}_2^t)_4]\}$  **10c**, identified by its diagnostic low-field NMR signal for the  $sp^2$ -Si atom (244.9 ppm). The THF-ligand in the zirconium silylene complex **10a** can be also readily exchanged with the  $\text{Me}_3P$ -ligand forming a new complex  $\{Cp_2Zr(\text{PMe}_3)=\text{Si}[Si_3(\text{SiMeBu}_2^t)_2]\}$  **10b**, also possessing strongly deshielded  $sp^2$ -Si center (282.1 ppm) (see Scheme 7).<sup>23,30</sup>

Based on their properties, both experimental [ $\delta$  ( $^{29}\text{Si}$  NMR) and Zr-Si bond length] and calculated [NPA atomic charges and WBI for the titanium–silicon bond], all complexes **10a**, **10b** and **10c** are also classified as Schrock-type zirconium silylenes  $\text{Zr}^{\delta+}=\text{Si}^{\delta-}$ . Accordingly, the reactivity of these complexes towards methanol is in line with this bond polarization to form the product **12**, identical to the one obtained by the methanolysis of titanium silylenes **9a,b** (see Scheme 8).

### 2.1.3. Hafnium silylides Hf=Si

The very first isolable hafnium silylene complex with  $\text{Hf}=\text{Si}$  double bond, 18-electron  $\{\text{Cp}_2^*(\text{PMe}_3)\text{Hf}=\text{Si}(\text{SiMeBu}_2^l)_2\}$  **16**, was synthesized by the reaction of 1,1-dilithiosilane  $(\text{Bu}_2^l\text{MeSi})_2\text{SiLi}_2$  with hafnocene dichloride  $\text{Cp}_2^*\text{HfCl}_2$ , generating at first metastable 16-electron complex  $\{\text{Cp}_2^*\text{Hf}=\text{Si}(\text{SiMeBu}_2^l)_2\}$  followed by its stabilization by complexation with  $\text{PMe}_3$  (Scheme 12, E = Si).<sup>34</sup>



**Scheme 12** Synthesis of the hafnium silylene complex **16** and hafnium germylene complex **17**.

The two  $\text{Cp}'$ -substituents on hafnium and  $\text{Bu}_2^1\text{MeSi}$ -substituents on silicon are non-equivalent in the NMR spectra of **16**, testifying for the lack of the free rotation about the  $\text{Hf}=\text{Si}$  double bond. The silylene center in **16** expectedly resonated at the remarkably low-field (295.4 ppm; d,  $^2J_{\text{Si}-\text{P}} = 15.0$  Hz), as is typical for the base-free transition metal–silylene complexes. Crystallographically, the hafnium–silicon bond of 2.6515(9) Å in **16** is markedly squeezed, being *ca.* 5% shorter than those of the related complexes with the  $\text{Hf}=\text{Si}$  single bond, and the geometry around the  $\text{sp}^2$ -silicon center is practically planar.

with  $\Sigma_{\text{Si}} = 359.8^\circ$ . The NPA calculations disclosed strong polarization of the  $\text{Hf}=\text{Si}$  double bond: hafnium is positively charged (+0.78), whereas silicon is charged negatively (-0.34) [ $\{\text{Cp}_2^*(\text{PMe}_3)\text{Hf}=\text{Si}(\text{SiMe}_3)_2\}$  model, DFT B3LYP/6-31G(d) for the P, Si, C, and H atoms and LANL2DZ for the Hf atom]. Such characteristic  $\text{Hf}^{\delta+}=\text{Si}^{\delta-}$  double bond polarization in **16** allows for its classification as the Schrock-type hafnium silylidene, as the first ever reported Schrock-type transition metal silylene complex.<sup>34</sup>

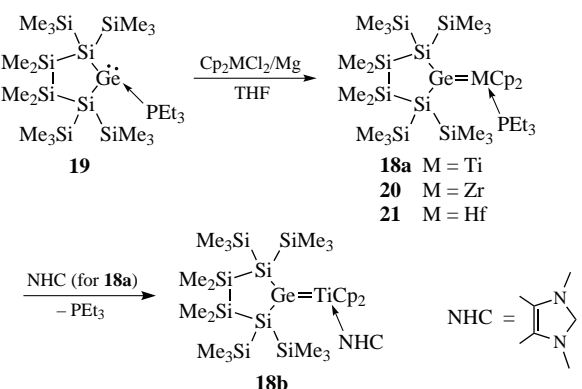
By the synthetic strategy previously successfully applied for the synthesis of the above-described titanium and zirconium silylenes **9a**, **10a** and **10c**, hafnium silylene complexes  $\{\text{Cp}_2\text{Hf}(\text{thf})=\text{Si}[\text{Si}_3(\text{SiMeBu}_2^{\ddagger})_4]\}$  **11a** and  $\{\text{Cp}_2\text{Hf}(\text{thf})=\text{Si}[\text{Si}_3(\text{SiMeBu}_2^{\ddagger})_4]\}$  **11c** were also readily available by the reaction of the calcium salt **8a** with hafnocene dichlorides (see Scheme 7,  $M = \text{Hf}$ ).<sup>23,30</sup> Ligand exchange converted hafnium THF-complex  $\{\text{Cp}_2\text{Hf}(\text{thf})=\text{Si}[\text{Si}_3(\text{SiMeBu}_2^{\ddagger})_4]\}$  **11a** to the hafnium-phosphine complex  $\{\text{Cp}_2\text{Hf}(\text{PMe}_3)=\text{Si}[\text{Si}_3(\text{SiMeBu}_2^{\ddagger})_4]\}$  **11b**. All hafnium complexes **11a**, **11b** and **11c** uniformly revealed strongly deshielded  $\text{sp}^2\text{-Si}$  centers, which resonances were observed at 214.6, 212.1 and 250.3 ppm, respectively.<sup>23,30</sup> Accordingly, all of them were safely categorized as Schrock-type hafnium silylenes  $\text{Hf}^{\delta^+}=\text{Si}^{\delta^-}$ , which was supported by the NPA charge calculations and specific reactivity towards methanol [the same as that of the above-described titanium and zirconium silylenes (see Scheme 8)].

## 2.2. Group 4 metal germylidenes

### 2.2.1. Titanium germylidenes $Ti=Ge$

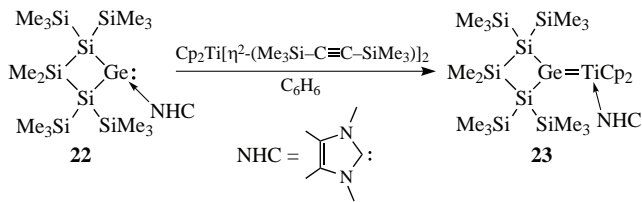
There are very few isolable titanium germylene complexes that were reported to date. It comes as no surprise given the intrinsically weak  $\text{Ti}=\text{Ge}$  double bond caused by: (1) weakness of the  $\text{Ti}-\text{Ge}$  single bond, due to the comparable sizes of  $3d(\text{Ti})$ - and  $3p(\text{Ti})$ -shells and the resulting Pauli repulsion between the occupied  $3p(\text{Ti})$ -orbitals and donor orbitals of the germylene ligand;<sup>35,36</sup> (2) poor ability of the titanium for  $\pi$ -bonding due to the spatial and energetic mismatch between the  $3d(\text{Ti})$ - and  $4p(\text{Ge})$ -orbitals.<sup>37</sup>

The first titanium germylene complex **18a**, as its PEt<sub>3</sub>-adduct, was synthesized by Marschner and co-workers by the reduction of titanocene dichloride with magnesium in the presence of the five-membered ring cyclic germylene-PEt<sub>3</sub> complex **19** (Scheme 13).<sup>37</sup> The ligand exchange with NHC converted **18a** to the NHC-complex **18b** (see Scheme 13, NHC = 1,3,4,5-tetra-methylimidazol-2-ylidene).<sup>37</sup>



**Scheme 13** Synthesis of the titanium-, zirconium- and hafnium germylene complexes **18a**, **18b**, **20** and **21**.

Reaction of the four-membered ring cyclic germylene–NHC complex **22** with  $\{\text{Cp}_2\text{Ti}[\eta^2-(\text{Me}_3\text{Si}-\text{C}\equiv\text{C}-\text{SiMe}_3)]_2\}$  (as a ‘ $\text{Cp}_2\text{Ti}$ ’ precursor) formed NHC-stabilized titanium germylene complex **23** (Scheme 14).<sup>37</sup>

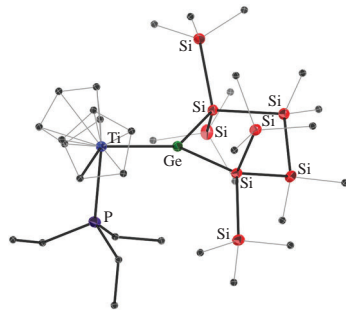
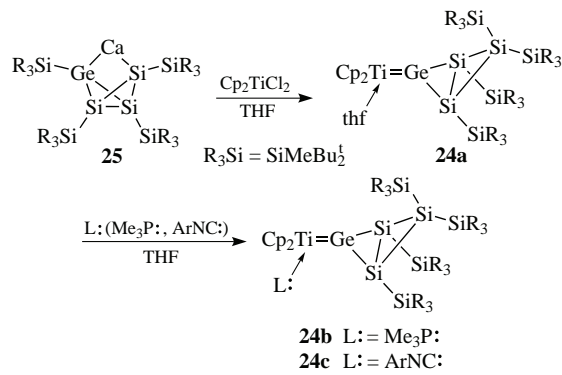


Scheme 14 Synthesis of the titanium germylene complex 23.

In the titanium–germylene complexes **18a** and **18b**, the  $\text{Si}_4\text{Ge}$  five-membered ring is nearly orthogonal to the metallocene equatorial plane, which allowed for an effective  $\pi$ -back-bonding from the filled  $d$ -orbital(Ti) to the vacant  $p$ -orbital(Ge) (Figure 4). The titanium–germanium bonds are short, 2.536(1) Å (in **18a**) and 2.5217(8) Å (in **23**), being notably shorter than the Ti–Ge single bonds in the previously reported titanium–germyl complexes, and the  $\text{sp}^2$ -Ge centers revealed nearly ideal trigonal-planar geometry with  $\Sigma_{\text{Ge}} = 359.9^\circ$  (in **18a**) and  $358.4^\circ$  (in **23**). The longest wavelength absorption in the titanium germylene complexes was observed at 531 nm (in **18a**) and 552 nm (in **23**), attributed to a blend of  $\pi$ – $\pi^*$  and  $\pi$ – $\sigma^*$  electronic transitions (in **18a**).

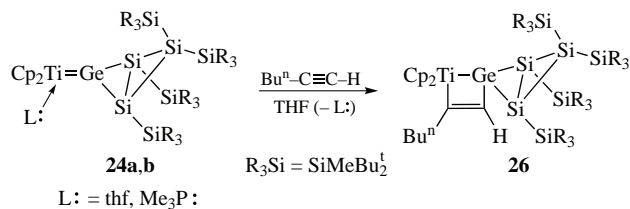
The doubly-bonded nature of the titanium–germanium bond in these complexes was supported by computations [DFT M06-2X/SDD (Ge, Ti, Zr, Hf), 6-31G(d) (P, Si, C, H)], which showed high WBI value of 1.54 (for **18a**). This value, however, was smaller than those for the isostructural zirconium and hafnium germylene complexes **20** and **21** (for their structures, see below) of 1.66 and 1.64, respectively. This is in line with the calculated bond dissociation energies (BDE) for the M=Ge bond (M = Ti, Zr, Hf): 42.3 kcal mol<sup>-1</sup> (for Ti=Ge bond in **18a**) vs. 65.9 kcal mol<sup>-1</sup> (for Zr=Ge bond in **20**) vs. 71.7 kcal mol<sup>-1</sup> (for Hf=Ge bond in **21**). That is, the strength of the M=Ge double bond (M = Ti, Zr, Hf) increases from Ti to Zr to Hf. In all these germylene complexes **18a**, **20** and **21**, the M=Ge bond is best described by the conventional  $\sigma$ -bonding/ $\pi$ -back-bonding interaction scheme typical for carbene complexes. However, the extent of  $\pi$ -back-bonding is smallest for the titanium germylene complex **18a** and largest for the hafnium germylene complex **21**. The attractive dispersion forces, responsible for the noncovalent van der Waals interactions, are of critical importance for the overall M=Ge binding energy. Thus, it accounts for 55% of the overall BDE (for **18a**) and to 42% (for **21**). Although no definite assignment of the complexes **18a**, **18b** and **23** to either Fischer- or Schrock-type complexes has been made, based on their peculiar substitution pattern it is reliable to assign them as the Schrock-type germylidene.

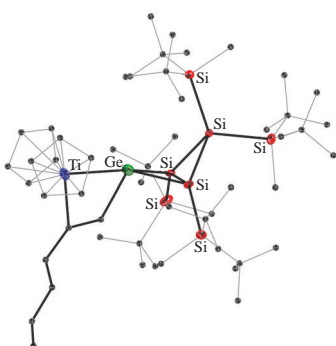
The second isolable titanium germylene complex,  $\{\text{Cp}_2\text{Ti}(\text{thf})=\text{Ge}[\text{Si}_3(\text{SiMeBu}_2^t)_4]\}$  **24a**, was prepared by the synthetic procedure preliminarily successfully applied for the preparation of isostructural titanium silylene complex **9a**,<sup>29</sup> namely, by the reaction of the calcium salt of 1,2,3-trisila-4-germabicyclo[1.1.0]butane-2,4-diide **25** with titanocene dichloride (Scheme 15).<sup>26</sup>

Figure 4 Crystal structure of the titanium germylene  $\text{Et}_3\text{P}$ -complex **18a**.Scheme 15 Synthesis of the titanium germylene complexes **24a–c**.

The initially formed 18-electron THF-complex **24a** was highly unstable decomposing in solution at room temperature in a matter of an hour, which precluded its isolation in a pure form. As in the case of the above-described titanium silylene THF-complex **9a**, the decomposition of **24a** involved ready dissociation of the loosely coordinated THF-ligand and generation of the intrinsically unstable coordinatively unsaturated 16-electron complex  $\{\text{Cp}_2\text{Ti}=\text{Ge}[\text{Si}_3(\text{SiMeBu}_2^t)_4]\}$ , that was remarkably destabilized compared to its silicon analogue  $\{\text{Cp}_2\text{Ti}=\text{Si}[\text{Si}_3(\text{SiMeBu}_2^t)_4]\}$ . However, using stronger coordinating Lewis base ligands (trimethylphosphine or xylyl isocyanide), titanium germylene complexes **24b** and **24c** were readily isolated being indefinitely stable both in the solid state and in solution (see Scheme 15).<sup>26</sup> In both **24b** and **24c**, the doubly-bonded germanium center is tricoordinate and planar with  $\Sigma_{\text{Ge}} = 359.6^\circ$  and  $359.2^\circ$ , respectively, and the titanium–germanium bond is remarkably short [2.5387(3) and 2.5276(3) Å, respectively], being very similar to those of Marschner's titanium germylene complexes **18a** [2.536(1) Å]<sup>37</sup> and **23** [2.5217(8) Å]<sup>37</sup> and much shorter than the Ti–Ge single bonds in the reported titanium germyl complexes [2.652(2)–2.710(2) Å]. In **24c**, the isocyanide ligand coordinates to Ti nearly perpendicularly ( $\text{C}_{\text{isocyanide}}\text{-Ti-Ge}$  bond angle is  $89^\circ$ ), whereas in **24b** bulkier phosphine ligand coordinates to Ti at a wider angle ( $\text{P}_{\text{phosphine}}\text{-Ti-Ge}$  bond angle is  $96^\circ$ ).

The NPA charges derived from the electrostatic potential [CHarges from Electrostatic Potentials using a Grid-based method (CHELPG) calculation scheme]<sup>38</sup> testified for a remarkable polarization of the titanium–germanium bond: +0.42 for Ti and -0.37 for Ge (in the hypothetical ligand-free complex  $\{\text{Cp}_2\text{Ti}=\text{Ge}[\text{Si}_3(\text{SiMeBu}_2^t)_4]\}$ ), +0.31 for Ti and -0.24 for Ge (in THF-complex **24a**), +0.15 for Ti and -0.32 for Ge (in  $\text{Me}_3\text{P}$ -complex **24b**), and +0.29 for Ti and -0.21 for Ge (in XylylNC-complex **24c**). Accordingly, both **24b** and **24c** should be formulated as the Schrock-type titanium germylidene featuring predominantly covalent  $\text{Ti}^{\delta+}=\text{Ge}^{\delta-}$  double bond with the nucleophilic Ge center (Lewis base) and electrophilic  $\text{Ti}^{\text{IV}}$  center (Lewis acid) in its highest oxidation state ( $d^0$ ). In line with the general trend of weakening of the Ti=E bonds (E = Si, Ge, Sn, Pb) descending group 14, the BDE of the Ti=Ge bond in **24b** (22.5 kcal mol<sup>-1</sup> based on the reaction enthalpy or

Scheme 16 [2+2] Cycloaddition of the titanium germylidene **24a,b** and 1-hexyne forming germatitanacyclobutene **26**.



**Figure 5** Crystal structure of the germatitanacyclobutene **26**.

26.1 kcal mol<sup>−1</sup> based on the reaction energy) is expectedly smaller than the BDE calculated for the Ti=Si bond in the isostructural titanium silylidene complex **9b** (23.9 kcal mol<sup>−1</sup> based on the reaction enthalpy or 27.7 kcal mol<sup>−1</sup> based on the reaction energy). Similar to the isostructural titanium silylidenes **9a–c**, titanium germylidenes **24a,b** also smoothly undergo [2+2] cycloaddition with the terminal alkynes forming the corresponding metallacycles, germatitanacyclobutene derivatives (for the reaction with 1-hexyne, see Scheme 16 and Figure 5).

### 2.2.2. Zirconium germylidenes Zr=Ge

The only currently known zirconium germylene complex **20** was reported by Marschner and co-workers, prepared by the same methodology applied for the synthesis of its titanium congener **18a**, namely by the co-reduction of zirconocene dichloride and cyclic germylene **19** with magnesium (see Scheme 13, M = Zr).<sup>37</sup> The Zr=Ge bond of 2.632(1) Å in **20** is notably shorter than the currently known Zr–Ge single bonds, and the Ge center exhibited trigonal-planar configuration with  $\Sigma_{\text{Ge}} = 359.6^\circ$ , thus proving a multiple bond character of the zirconium–germanium bond. The longest wavelength UV-absorption in **20** was found at 507 nm, being assigned to the  $\pi_{\text{Zr=Ge}}-\pi^*_{\text{Zr=Ge}}$  electronic transition. Based on its characteristics, complex **20** should also be classified as the Schrock-type zirconium germylidene.

### 2.2.3. Hafnium germylidenes Hf=Ge

Marschner and co-workers prepared also hafnium germylene complex **21**, applying the synthetic strategy successfully used for the preparation of its lighter homologues **18a** and **20**: co-reduction of hafnocene dichloride and cyclic germylene **19** with magnesium (see Scheme 13, M = Hf).<sup>37</sup> The multiple bond nature of the hafnium–germanium bond in **21** was reliably proved by its bond length of 2.600(1) Å that was significantly shorter than the previously reported Hf–Ge single bonds, and trigonal-planar geometry at the sp<sup>2</sup>–Ge atom with  $\Sigma_{\text{Ge}} = 359.6^\circ$ . The longest wavelength UV-absorption (502 nm,  $\pi_{\text{Hf=Ge}}-\pi^*_{\text{Hf=Ge}}$ ) of the hafnium germylene complex **21** is closer to that of its zirconium congener **20** (507 nm) than to that of its titanium analogue **18a** (531 nm). This novel Hf=Ge complex **21** should also be identified as the Schrock-type hafnium germylidene.

The second reported example of an isolable hafnium germylene complex, *viz.* 18-electron  $\{\text{Cp}_2^{\text{t}}(\text{PMe}_3)\text{Hf=Ge}(\text{SiMeBu}_5^{\text{t}})_2\}$  **17**, was synthesized similarly to its above-described silicon analogue **16** by the reaction of  $\text{Cp}_2^{\text{t}}\text{HfCl}_2$  with  $(\text{Bu}_2^{\text{t}}\text{MeSi})_2\text{GeLi}_2$  *via* the transient 16-electron complex  $\{\text{Cp}_2^{\text{t}}\text{Hf=Ge}(\text{SiMeBu}_5^{\text{t}})_2\}$  followed by the subsequent stabilization of the latter by  $\text{PMe}_3$  (see Scheme 12, E = Ge).<sup>39</sup> In accord with formulation of the Hf=Ge double bond, Cp<sup>t</sup>-substituents and silyl-substituents on the Hf and Ge centers, respectively, are non-equivalent in the NMR spectra of **17**. The geometry around the sp<sup>2</sup>–Ge center in **17** is nearly ideal trigonal-planar with  $\Sigma_{\text{Ge}} = 359.8^\circ$ , and the hafnium–germanium bond of 2.6705(5) Å is notably short, being

3–7% shorter than those in the structurally authenticated compounds with the Hf–Ge single bonds, although slightly longer than the Hf=Ge bond in Marschner's complex **21**<sup>37</sup> [2.600(1) Å]. The presence of the Hf=Ge double bond in **17** was further substantiated by its UV measurement: the longest wavelength absorption at 501 nm was assigned to the  $\pi_{\text{Hf=Ge}}-\pi^*_{\text{Hf=Ge}}$  HOMO–LUMO electronic transition. The NPA charges of the model compound  $\{\text{Cp}_2^{\text{t}}(\text{PMe}_3)\text{Hf=Ge}(\text{SiMe}_3)_2\}$  disclosed strong polarization of the Hf=Ge bond: +0.74 (Hf) and −0.32 (Ge). This remarkable  $\text{Hf}^{\delta+}=\text{Ge}^{\delta-}$  bond polarization is in accord with the formulation of **17** as the Schrock-type germylidene featuring electrophilic hafnium center in its highest oxidation state (*d*<sup>0</sup>) and profoundly nucleophilic germanium center.

### 3. Conclusions

As was mentioned in the final part of Introduction, to develop silicon (or germanium) versions of metathesis, one needs to find a way to generate metallacyclobutanes (in the case of olefin metathesis) or metallacyclobutenes (in the case of enyne metathesis) as the key reaction intermediates of the whole catalytic cycle. By synthesizing Schrock-type silylidenes and germylidenes of the group 4 metals, capable of the [2+2] cycloadditions with unsaturated substrates to form the desired metallacycles, this problem has been partially solved. However, such metallacycles **14a–c** (see Scheme 9) and **26** (see Scheme 16) were still unable to undergo ring-opening isomerization to intermediate dimetalladienes  $\text{Ti}=\text{C}=\text{C}=\text{E}$  (E = Si, Ge) followed by the second [2+2] cycloaddition of their Ti=C bond with alkene generating metallacyclobutane with its subsequent thermal cycloelimination to form finally metalladienes  $>\text{C}=\text{C}=\text{C}=\text{E}<$  (E = Si, Ge) as the desired end products. Evidently, for the further progress of the silicon (or germanium) metathesis catalytic cycle, one needs to develop novel Schrock-type silylidenes and germylidenes of the early and mid-transition metals (as only these metals are expected to produce Schrock-type complexes), that can readily undergo [2+2] cycloaddition with a variety of unsaturated organic substrates forming corresponding metallacycles that are capable of the subsequent cycloelimination. As an alternative to the above-described process, of paramount importance would be the development of the metathesis involving *in situ* generation of the highly reactive Schrock-type silylidenes and germylidenes (from the readily available and easy-to-handle starting materials) which would instantly react with alkenes or alkynes already presented in the reaction system to initiate the catalytic cycle. This perspective is especially attractive and important from the technological viewpoint as a potential alternative source for the highly desirable, but otherwise hardly available, Si- and Ge-containing unsaturated derivatives. The latter might serve as the immediate precursors for a plethora of the advanced materials of the new generation, such as polymers, ceramics, nanocomposites, *etc.* The constantly growing and highly productive research in the field of silylene and germylene transition metal complexes gives a hope that the fast and remarkable progress can be achieved in the observable future.

This work is partially supported by the JSPS KAKENHI Grants program (no. JP21K05017) from the Ministry of Education, Science, Sports, and Culture of Japan.

### References

- 1 *Handbook of Metathesis*, ed. R. H. Grubbs, Wiley–VCH, Weinheim, 2003, vols. 1–3.
- 2 R. H. Grubbs, *Tetrahedron*, 2004, **60**, 7117.
- 3 D. Astruc, *New J. Chem.*, 2005, **29**, 42.

4 Y. Chauvin, *Angew. Chem., Int. Ed.*, 2006, **45**, 3741.

5 R. R. Schrock, *Angew. Chem., Int. Ed.*, 2006, **45**, 3748.

6 R. H. Grubbs, *Angew. Chem., Int. Ed.*, 2006, **45**, 3760.

7 J. C. Mol, *J. Mol. Catal. A: Chem.*, 2004, **213**, 39.

8 *Metathesis in Natural Product Synthesis: Strategies, Substrates and Catalysts*, eds. J. Cossy, S. Arseniyadis and C. Meyer, Wiley–VCH, Weinheim, 2010, vols. 1–3.

9 P. Schwab, M. B. France, J. W. Ziller and R. H. Grubbs, *Angew. Chem., Int. Ed. Engl.*, 1995, **34**, 2039.

10 P. Schwab, R. H. Grubbs and J. W. Ziller, *J. Am. Chem. Soc.*, 1996, **118**, 100.

11 M. Scholl, S. Ding, C. W. Lee and R. H. Grubbs, *Org. Lett.*, 1999, **1**, 953.

12 J. A. Love, J. P. Morgan, T. M. Trnka and R. H. Grubbs, *Angew. Chem., Int. Ed.*, 2002, **41**, 4035.

13 J. S. Kingsbury, J. P. A. Harrity, P. J. Bonitatebus, Jr. and A. H. Hoveyda, *J. Am. Chem. Soc.*, 1999, **121**, 791.

14 S. B. Garber, J. S. Kingsbury, B. L. Gray and A. H. Hoveyda, *J. Am. Chem. Soc.*, 2000, **122**, 8168.

15 S. Gessler, S. Rndl and S. Blechert, *Tetrahedron Lett.*, 2000, **41**, 9973.

16 R. R. Schrock, J. S. Murdzek, G. C. Bazan, J. Robbins, M. DiMare and M. O'Regan, *J. Am. Chem. Soc.*, 1990, **112**, 3875.

17 J.-L. Hérisson and Y. Chauvin, *Makromol. Chem.*, 1971, **141**, 161.

18 W. Petz, *Chem. Rev.*, 1986, **86**, 1019.

19 M. F. Lappert and R. S. Rowe, *Coord. Chem. Rev.*, 1990, **100**, 267.

20 P. D. Lickiss, *Chem. Soc. Rev.*, 1992, **21**, 271.

21 H. Ogino, *Chem. Rec.*, 2002, **2**, 291.

22 R. Waterman, P. G. Hayes and T. Don Tilley, *Acc. Chem. Res.*, 2007, **40**, 712.

23 V. Ya. Lee, *Eur. J. Inorg. Chem.*, 2022, e202200175.

24 T. J. Hadlington, A. Kostenko and M. Driess, *Chem. – Eur. J.*, 2020, **26**, 1958.

25 K. Takanashi, V. Ya. Lee, T. Yokoyama and A. Sekiguchi, *J. Am. Chem. Soc.*, 2009, **131**, 916.

26 V. Ya. Lee, R. Sakai, K. Takanashi, O. A. Gapurenko, R. M. Minyaev, H. Gornitzka and A. Sekiguchi, *Angew. Chem., Int. Ed.*, 2021, **60**, 3951.

27 G. Chung and M. S. Gordon, *Organometallics*, 2003, **22**, 42.

28 B. Blom, M. Driess, D. Gallego and S. Inoue, *Chem. – Eur. J.*, 2012, **18**, 13355.

29 V. Ya. Lee, S. Aoki, T. Yokoyama, S. Horiguchi, A. Sekiguchi, H. Gornitzka, J.-D. Guo and S. Nagase, *J. Am. Chem. Soc.*, 2013, **135**, 2987.

30 T. Yokoyama, *Master (MSc) Thesis*, University of Tsukuba (Japan), 2010.

31 G. P. Mitchell and T. Don Tilley, *J. Am. Chem. Soc.*, 1997, **119**, 11236.

32 V. Ya. Lee, O. A. Gapurenko, V. I. Minkin, S. Horiguchi and A. Sekiguchi, *Russ. Chem. Bull.*, 2016, **65**, 1139.

33 V. Ya. Lee, S. Horiguchi, O. A. Gapurenko, R. M. Minyaev, V. I. Minkin, H. Gornitzka and A. Sekiguchi, *Eur. J. Inorg. Chem.*, 2019, 4224.

34 N. Nakata, T. Fujita and A. Sekiguchi, *J. Am. Chem. Soc.*, 2006, **128**, 16024.

35 M. Kaupp, *J. Comput. Chem.*, 2006, **28**, 320.

36 M. A. Buijse and E. J. Baerends, *J. Chem. Phys.*, 1990, **93**, 4129.

37 J. Hlina, J. Baumgartner, C. Marschner, P. Zark and T. Müller, *Organometallics*, 2013, **32**, 3300.

38 C. M. Breneman and K. B. Wiberg, *J. Comput. Chem.*, 1990, **11**, 361.

39 N. Nakata, S. Aoki, V. Ya. Lee and A. Sekiguchi, *Organometallics*, 2015, **34**, 2699.

Received: 4th October 2022; Com. 22/7010